# Optimum Design of Maxwell-type Damper System Based on Stochastically Equivalent Damping Factor

**S. Matsuda**
*Kansai University, Japan*

**SUMMARY**
The purpose of this study is to develop a method for finding the optimal configuration of Maxwell-type dampers which maximize the equivalent damping factor of a multi-degrees-of-freedom structural system. The equivalent damping factor defined by the energy-consuming ratio is evaluated stochastically based on the energy response of the structural system under a stationary random excitation. In this study, two types of random excitation models are considered: a white noise with a flat spectrum and a filtered noise with one predominant frequency. It is shown that the optimal distribution of the damping coefficients is closely proportional to that of the stiffness of the Maxwell elements. The effectiveness of the optimized damper system is also demonstrated through the response analysis for several observed earthquake excitations.

*Keywords: Maxwell-type damper, Optimum design, Equivalent damping factor, Random response analysis*

## 1. INTRODUCTION

The Maxwell-type damper represents in this study a type of a supplemental damper which can be modeled as the Maxwell element consisting of a spring and a dashpot in a series. A viscous or visco-elastic damper installed with an elastic brace, for example, can be expressed and analyzed by using this Maxwell-type damper model (Hatada et al. 2000, Singh et al. 2003, Chen et al. 2010). Since the performance of the Maxwell-type damper could be reduced by the softness of its spring element, it has been an important issue to design the Maxwell-type dampers installed in a structure so as to maximize their performances. In this point of view, the purpose of this study is to develop a method for finding the optimal configuration of the Maxwell-type dampers which maximize the equivalent damping factor of a multi-degrees-of-freedom structural system. The equivalent damping factor is selected as the objective function of the optimization problem and evaluated by the energy-consuming ratio for the stationary response process of the structural system subjected to stationary random ground excitations. It is expected that response indices of all stories and all modes are weighted automatically and summarized to the equivalent damping factor based on their contributions to the energy dissipation of the whole structural system. In this study, two types of inputs given as white and non-white stationary random excitations are considered and compared each other on the effectiveness of the dampers optimized for them. Furthermore, the effectiveness is also examined for several non-stationary excitations of observed ground motions.

## 2. FORMULATION

The $N$-story structural model investigated in this study is shown in Fig. 1. $M_i, K_i$ and $C_i$ denote the mass, the stiffness, and the inherent damping coefficient of the $i$th story, respectively. The viscous damper installed in the $i$th story is modeled as a Maxwell element consisted of a spring with a stiffness $K_{Di}$ and a serially connected dashpot with a damping coefficient $C_{Di}$. Let $X_i(t)$ denote the relative displacement of the $i$th story with respect to the base, and $Y_i(t) - Y_{i-1}(t)$ denote the elongation of the spring in the $i$ th Maxwell element as shown in Fig. 1.

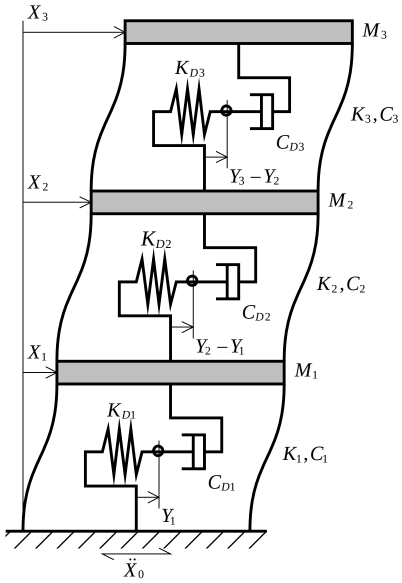


**Figure 1.** $N$ -story structural model with Maxwell dampers

The equation of motion for the structural model subjected to a ground-level excitation $\ddot{X}_0(t)$ is given by

$$[M]\{\ddot{X}\}+[C]\{\dot{X}\}+[K]\{X\}+[K_D]\{Y\}=-[M]\{1\}\ddot{X}_0 \tag{2.1}$$

where $[M],[K]$ and $[C]$ represent the mass, the stiffness and the damping matrices, respectively, in the relative coordinate system with respect to the base; $[K_D]$ is the stiffness matrix made by replacing $K_i$ in $[K]$ with $K_{Di}$; $\{X\}$ and $\{Y\}$ are row vectors with components $X_i$ and $Y_i$, respectively; and $\{1\}$ is a vector whose components are all unity. A dot over a quantity indicates the time derivative. The restoring force of the spring $K_{Di}$ balances with the damping force generated by the dashpot $C_{Di}$. This relation can be expressed by the following equation:

$$[K_D]\{Y\}=[C_D](\{\dot{X}\}-\{\dot{Y}\}) \tag{2.2}$$

where $[C_D]$ is the damping matrix made by replacing $K_{Di}$ in $[K_D]$ with $C_{Di}$. In the state space composed of the state vector $\{Z\}^T=\{\{X\}^T \quad \{\dot{X}\}^T \quad \{Y\}^T\}^T$, Eqns. (2.1) and (2.2) are combined together and give the following differential equation:

$$\{\dot{Z}\}=[A]\{Z\}+\{B\} \tag{2.3}$$

where

$$[A]=\left[\begin{array}{c|c|c} [0] & [I] & [0] \\ \hline -[M]^{-1}[K] & -[M]^{-1}[C] & -[M]^{-1}[K_D] \\ \hline [0] & [I] & -[C_D]^{-1}[K_D] \end{array}\right],\{B\}=\left\{\begin{array}{c} \{0\} \\ \hline -\{1\}\ddot{X}_0 \\ \hline \{0\} \end{array}\right\} \tag{2.4}$$

and $[I]$ is the identity matrix. Assuming that the input ground motion $\ddot{X}_0(t)=W(t)$ is a stationary white noise (WN) with zero mean and a constant power spectral density $S_0$, the variance-covariance matrix of $\{Z\}$ given by $[\Sigma_{ZZ}]=E[\{Z\}\{Z\}^T]$ obeys the following equation (Matsuda et al. 2006):

$$[\dot{\Sigma}_{ZZ}]=[A][\Sigma_{ZZ}]+[\Sigma_{ZZ}][A]^T+[B] \tag{2.5}$$

where

$$[B] = E[\{B\}\{Z\}^T + \{Z\}^T\{B\}] = \begin{bmatrix} [0] & [0] & [0] \\ [0] & [S_0] & [0] \\ [0] & [0] & [0] \end{bmatrix} \tag{2.6}$$

and $[S_0]$ is a matrix whose elements are all $S_0$. The operator $E$ means the ensemble average. When the stationary response process is considered, the left-hand side of Eqn. (2.5) converges to zero and $[\Sigma_{ZZ}]$ can be obtained by solving the following matrix linear equation:

$$[A][\Sigma_{ZZ}] + [\Sigma_{ZZ}][A]^T + [B] = [0] \tag{2.7}$$

The equilibrium equation of energy for the structural system can be obtained by the integration of the scalar product of Eqn. (2.1) in both-hand sides with the velocity vector $\{\dot{X}\}$ with respect to time over the duration $T_D$:

$$\int_0^{T_D} \{\dot{X}\}^T \left([M]\{\ddot{X}\} + [C]\{\dot{X}\} + [K]\{X\} + [K_D]\{Y\}\right) dt = -\int_0^{T_D} \{\dot{X}\}^T [M]\{1\}\ddot{X}_0 dt \tag{2.8}$$

By using Eqn. (2.2), we can simplify Eqn. (2.8) as follows:

$$(E_K + E_P)\Big|_{t=0}^{t=T_D} + {}_F E_D + {}_D E_D = E_I \tag{2.9}$$

where

$$\begin{aligned} &E_K = \frac{1}{2}\{\dot{X}\}^T[M]\{\dot{X}\}, \quad E_P = \frac{1}{2}\{X\}^T[K]\{X\} + \frac{1}{2}\{Y\}^T[K_D]\{Y\}, \\ &{}_F E_D = \int_0^{T_D} \{\dot{X}\}^T[C]\{\dot{X}\}dt, \quad {}_D E_D = \int_0^{T_D} (\{\dot{X}\} - \{\dot{Y}\})^T[C_D](\{\dot{X}\} - \{\dot{Y}\})dt, \\ &E_I = -\int_0^{T_D} \{\dot{X}\}^T[M]\{1\}\ddot{X}_0 dt \end{aligned} \tag{2.10}$$

$E_K$, $E_P$, ${}_F E_D$, ${}_D E_D$, and $E_I$ represent, the kinematic energy, the potential energy, the dissipated energy by the inherent viscous damping of the frame, that of by the Maxwell damper, and the earthquake input energy, respectively. Taking the ensemble average in stationary response of Eqn. (2.9) gives

$${}_F \overline{E}_D + {}_D \overline{E}_D = \overline{E}_I \tag{2.11}$$

where

$$\begin{aligned} &{}_F \overline{E}_D = T_D \cdot \sum_{i,j} (C)_{ij} E[\dot{X}_i \dot{X}_j], \\ &{}_D \overline{E}_D = T_D \cdot \sum_{i,j} (C_D)_{ij} E[(\dot{X}_i - \dot{Y}_i)(\dot{X}_j - \dot{Y}_j)] = T_D \cdot \sum_{i,j} (K_D)_{ij} E[\dot{X}_i Y_j], \\ &\overline{E}_I = -T_D \cdot \sum_i M_i E[\dot{X}_i \ddot{X}_0] = T_D \cdot (S_0 / 2) \sum_i M_i \end{aligned} \tag{2.12}$$

a bar over a quantity denotes the ensemble average of the quantity, and subscripts of parentheses indicate a component of the matrix. The variances and covariances in Eqn. (2.12) are given by the corresponding components of $[\Sigma_{ZZ}]$. The ensemble averages of $E_K$ and $E_P$ are given by

$$\overline{E}_K = \frac{1}{2}\sum_i M_i E[\dot{X}_i \dot{X}_i], \quad \overline{E}_P = \frac{1}{2}\sum_{i,j}\left((K)_{ij} E[X_i X_j] + (K_D)_{ij} E[Y_i Y_j]\right) \tag{2.13}$$

Since $\bar{E}_K(0) = \bar{E}_K(T_D) = const.$ and $\bar{E}_P(0) = \bar{E}_P(T_D) = const.$ in the stationary response, the first term of the left-hand side of Eqn. (2.9) vanishes in Eqn. (2.11).

The equivalent damping coefficient is evaluated by following formula:

$$h_{eq} = \Delta\bar{E} / (4\pi \bar{E}_{\max}) \tag{2.14}$$

where $\bar{E}_{\max}$ and $\Delta\bar{E}$ denote the average of maximum potential energy and the average of the dissipated energy in one cycle due to the damping, respectively. These two quantities are evaluated as follows:

$$\bar{E}_{\max} = \bar{E}_K + \bar{E}_P, \quad \Delta\bar{E} = ({}_F\bar{E}_D + {}_D\bar{E}_D) \times (T_{eq} / T_D) \tag{2.15}$$

where $T_{eq}$ is the equivalent natural period estimated by the following Rayleigh quotient:

$$T_{eq} = 2\pi \sqrt{\left(\sum_i M_i E[X_i X_i]\right) / \left(2\bar{E}_P\right)} \tag{2.16}$$

In this study, the equivalent damping factor $h_{eq}$ is selected as the performance index to be maximized by the optimization of the damper configuration. The two parameters characterizing the Maxwell damper in the $i$ th story, $K_{Di}$ and $C_{Di}$, are non-dimensionalized as follows:

$$\alpha_i = K_{Di} / K_i, \quad \beta_i = C_{Di} / 2\sqrt{M_i K_i} \tag{2.17}$$

where $\alpha_i$ and $\beta_i$ denote the non-dimensional stiffness coefficient and damping coefficient, respectively. The non-dimensional damping coefficients $\{\beta\}$ of installed Maxwell dampers are chosen as independent variables of the optimization problem. The optimal configuration of Maxwell dampers $\{\beta_{opt}\}$ is defined as that which maximizes the equivalent damping factor $h_{eq}$ under given non-dimensional stiffness coefficients $\{\alpha\}$. The $\{\beta_{opt}\}$ is obtained numerically by means of the quasi-Newton method.

The white noise $W(t)$ used as the input $\ddot{X}_0(t)$ with a constant power spectral density over an infinite bandwidth is ideal and easy to handle in analytical approaches. However, it is of course more natural to consider that ground motions have their own particular characteristics. To model and express such characteristics, we introduce another simple input ground motion model called as the pseudo-acceleration (PA) model (Matsuda 2006). The PA model is defined as a stationary pseudo-acceleration response process of a single-degree-of-freedom (SDOF) system with a natural angular frequency $\omega_g$ and a damping factor $h_g$ subjected to a white noise $W(t)$ with a constant power spectral density $S_0$. The input ground motion $\ddot{X}_0(t)$ is given by using the response process $X_g$ of the SDOF system as follows:

$$\ddot{X}_0(t) = \omega_g \cdot \dot{X}_g(t), \quad \ddot{X}_g + 2h_g\omega_g\dot{X}_g + \omega_g^2 X_g = -W(t) \tag{2.18}$$

The power spectral density function (PSDF) of the PA model is given by

$$S_{\ddot{X}_0}(\omega) = \frac{4h_g\omega_g\omega^2}{(\omega^2 - \omega_g^2)^2 + 4h_g^2\omega_g^2\omega^2}\sigma_g^2 \tag{2.19}$$

where $\sigma_g^2 = \omega_g S_0 / (4h_g) = E[\ddot{X}_0^2(t)]$. The PSDF $S_{\ddot{X}_0}(\omega)$ has one predominant frequency at around $\omega = \omega_g$ and its bandwidth is controlled by $h_g$. The response process of the $N$-story structural model subjected to the PA input motion model can be obtained by solving Eqns. (2.1) and (2.2) together with Eqn. (2.18). Introducing another extended state vector $\{Z\}^T = \{\{X\}^T \;\; \{\dot{X}\}^T \;\; \{Y\}^T \;\; X_g \;\; \dot{X}_g\}^T$, the same form of matrix equation as Eqn. (2.7) for the extended variance-covariance matrix $[\Sigma_{ZZ}]$ in the stationary response process is obtained, where the constant matrices $[A]$ and $[B]$ are replaced by

$$[A]=\left[\begin{array}{ccc|c|c} [0] & [I] & [0] & \{0\} & \{0\} \\ -[M]^{-1}[K] & -[M]^{-1}[C] & -[M]^{-1}[K_D] & \{0\} & -\omega_g\{1\} \\ [0] & [I] & -[C_D]^{-1}[K_D] & \{0\} & \{0\} \\ \hline \{0\}^T & \{0\}^T & \{0\}^T & 0 & 1 \\ \hline \{0\}^T & \{0\}^T & \{0\}^T & -\omega_g^2 & -2h_g\omega_g \end{array}\right],\quad [B]=\left[\begin{array}{c|c} [0] & \{0\} \\ \hline \{0\}^T & S_0 \end{array}\right] \tag{2.20}$$

The equivalent damping factor for the PA model input can also be obtained by Eqn. (2.14). Therefore, the optimal configuration of Maxwell dampers $\{\beta_{opt}\}$ can be defined and obtained in the same manner as for the case of the WN input described previously.

## 3. NUMERICAL RESULTS

The $N$-story structural model considered in this study is configured as follows: The masses $\{M\}$ are equal in all stories; The stiffness distribution $\{K\}$ with a given fundamental period $T_1$ is defined so as to induce an equal inter-story drift in all stories under static application of the shear forces for the seismic design in the Japanese Building Code (BCJ 2011); The damping coefficients $\{C\}$ are proportional to $\{K\}$ and have a certain damping factor for the first mode $h_1$. Table 1 shows the properties of a five-sotry structural model to be investigated hereafter in this study with $T_1 = 1.0$ [sec] and $h_1 = 0.02$.

**Table 1.** Properties of 5-story structural model

| $i$ | 1 | 2 | 3 | 4 | 5 |
|---|---|---|---|---|---|
| $M_i/M_1$* | 1.000 | 1.000 | 1.000 | 1.000 | 1.000 |
| $K_i/K_1$ (=$C_i/C_1$)* | 1.000 | 0.927 | 0.807 | 0.636 | 0.404 |
| $T_i$ [sec] | 1.000 | 0.393 | 0.251 | 0.188 | 0.151 |
| $h_i$ | 0.020 | 0.051 | 0.080 | 0.107 | 0.133 |

* $K_1/M_1$=577 [1/sec$^2$], $C_1/M_1$=3.68 [1/sec]

Figure 2 shows the relations between the non-dimensional damping coefficients $\{\beta\}$ and the corresponding equivalent damping factor $h_{eq}$ under the WN input. The dependences of $h_{eq}$ on $\beta_i$ are shown in Figure 2(a) for the cases that only one damper, for simplicity, is installed in the whole structural system with $\alpha_i = 0.5$. A damper installed in a lower story gives a higher $h_{eq}$ and a higher maximum of $h_{eq}$ with respect to $\beta_i$. The Figure 2(b) shows the effects on $h_{eq}$ of the stiffness $\alpha_1$ of a damper installed in the first story. A higher damping is achieved by a higher $\alpha_1$. It means that the spring of the Maxwell element with a higher stiffness can transmit a larger damping force to the frame and induce efficiently the damping effect. Although the $h_{eq}$ for other numbers and locations of dampers are omitted to show here, the same dependencies are observed on $\alpha_i$ and $\beta_i$: the $h_{eq}$ has a maximum with respect to each of $\beta_i$ and the maximum value increases with the increase of $\alpha_i$. This observation supports the possibility of the optimization of Maxwell dampers which maximize the damping factor of the structural system.

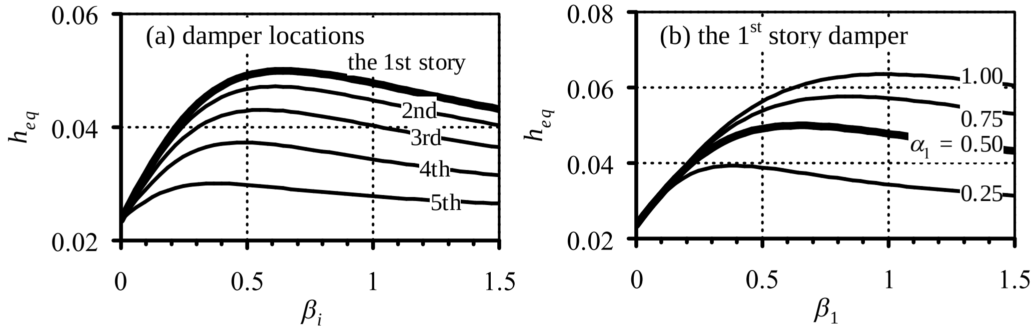


**Figure 2.** Dependence of equivalent damping factor on non-dimensional damping coefficient

Table 2 lists $\{\beta_{opt}\}$ for all possible locations of one or more (up to five) dampers and the corresponding damping factors of the five-story structural model subjected to the WN. In those cases, the non-dimensional stiffnesses $\{\alpha\}$ of Maxwell dampers are set to a constant value of $0.5$ for all stories. It is observed that a larger number of dampers can give a higher damping factor and lower stories are more efficient for the dampers to be installed in. Figure 3 shows the distribution of dampers and their effect on the structural response for the case of five dampers which give the maximum damping in Table 2. In Figure 3(a), the distribution of the optimal damping coefficients $\{\beta_{opt}\}$ is compared with that of the stifnesses of Maxwell dampers $\{K_D\}$. In this case, $\{\beta\}$ is almost proportional to $\{K_D\}$. It is reasonable because the springs of the Maxwell elements with higher stiffnesses can transmit larger damping forces. In Figure 3(d), the correlation between $\{\beta_{opt}\}$ and $\{K_D\}$ is examined for other random configurations of the structural parameters: one hundred sets of $T_1$ , $\{M\}$ , and $\{\alpha\}$ for five-story structural models are taken from uniform distributions of $\log_{10} T_1 \in [-1.0, 1.0]$, $M_i / M_1 \in [0.8, 1.2]$, and $\alpha_i \in [0.5, 1.5]$, respectively. There is observed a strong correlation between $\beta_i / \beta_1$ for the optimal configurations and $K_{Di} / K_{D1}$ with a correlation coefficient of 0.940. It could be possible to simplify the optimum problem by using the relation that $\{\beta_{opt}\}$ is closely proportional to $\{K_D\}$. Figure 3(b) and (c) show the reductions of the inter-story drifts and absolute accelerations, respectively, in analytically evaluated root-mean-square values compared with those of without dampers. The inter-story drifts are reduced by more than 50% in all stories. In absolute accelerations, the upper stories which have larger absolute accelerations without dampers get larger reductions. The maximum reduction, about 50%, is gained at the top story.

**Table 2.** Optimal damping coefficients of Maxwell dampers

| $n/N$ | $\beta_1$ | $\beta_2$ | $\beta_3$ | $\beta_4$ | $\beta_5$ | $h_{eq}$ | $n/N$ | $\beta_1$ | $\beta_2$ | $\beta_3$ | $\beta_4$ | $\beta_5$ | $h_{eq}$ |
|---|---|---|---|---|---|---|---|---|---|---|---|---|---|
| 5/5 | 0.729 | 0.663 | 0.591 | 0.487 | 0.321 | 0.122 | 2/5 | 0.652 | 0.617 | | | | 0.074 |
| 4/5 | 0.688 | 0.638 | 0.582 | 0.478 | | 0.111 | | 0.657 | | 0.571 | | | 0.070 |
| | 0.693 | 0.642 | 0.587 | | 0.322 | 0.105 | | | 0.616 | 0.567 | | | 0.066 |
| | 0.703 | 0.650 | | 0.488 | 0.334 | 0.099 | | 0.667 | | | 0.486 | | 0.065 |
| | 0.710 | | 0.578 | 0.481 | 0.341 | 0.094 | | | 0.629 | | 0.480 | | 0.061 |
| | | 0.650 | 0.574 | 0.477 | 0.335 | 0.090 | | 0.663 | | | | 0.360 | 0.057 |
| 3/5 | 0.658 | 0.619 | 0.577 | | | 0.094 | | | | 0.562 | 0.476 | | 0.057 |
| | 0.676 | 0.633 | | 0.486 | | 0.090 | | | 0.620 | | | 0.352 | 0.054 |
| | 0.688 | | 0.577 | 0.482 | | 0.085 | | | | 0.565 | | 0.360 | 0.050 |
| | 0.675 | 0.631 | | | 0.342 | 0.083 | | | | | 0.478 | 0.358 | 0.043 |
| | | 0.634 | 0.570 | 0.471 | | 0.081 | 1/5 | 0.648 | | | | | 0.050 |
| | 0.678 | | 0.578 | | 0.337 | 0.078 | | | 0.612 | | | | 0.047 |
| | | 0.627 | 0.572 | | 0.339 | 0.074 | | | | 0.562 | | | 0.043 |
| | 0.689 | | | 0.488 | 0.351 | 0.072 | | | | | 0.480 | | 0.037 |
| | | 0.635 | | 0.480 | 0.343 | 0.069 | | | | | | 0.369 | 0.030 |
| | | | 0.565 | 0.475 | 0.351 | 0.064 | 0/5 | | | | | | 0.023 |

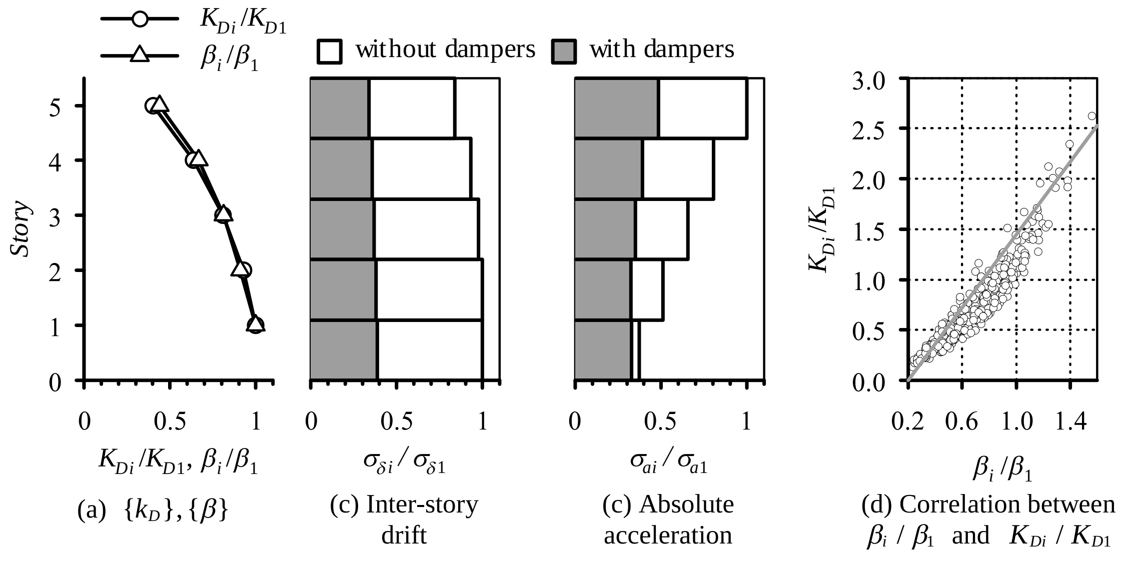


**Figure 3.** Distribution of optimal dampers and their effect on inter-story drifts and absolute accelerations

In Figure 3, the optimal dampers $\{\beta_{opt}\}$ designed for the WN input are investigated on their effectiveness under the same WN input. However, it is likely that the building with the dampers will experience ground motions with different characteristics from those of the assumed input motions in the process of their design. It is worth investigating the effectiveness of those dampers under the unexpected input motions. For this purpose, we use four observed ground motions: the acceleration records of Kobe (1995 Kobe earthquake), El Centro (1940 Imperial Valley earthquake), Hachinohe (1968 Tokachi-oki earthquake), and Takatsuki (2004 Kii-hanto-oki earthquake). All records are so standardized as to give a maximum velocity of 50 cm/sec. The PA models of stochastic input processes are also generated from those four records. The parameters of the PA models obtained by using the non-linear least square fitting method are listed in Table 3 and the corresponding PSDFs of the PA models are shown in Figure 4 together with those of the target records.

**Table 3.** Parameters of the PA models

| | $\sigma_g$ [cm/sec$^2$] | $\omega_g$ [rad/sec] | $T_g (=2\pi/\omega_g)$ [sec] | $h_g$ |
|---|---|---|---|---|
| (a) Kobe | 72.7 | 7.65 | 0.82 | 0.25 |
| (b) El Centro | 75.2 | 7.52 | 0.84 | 0.84 |
| (c) Hachinohe | 58.6 | 5.51 | 1.14 | 0.94 |
| (d) Takatsuki | 64.8 | 4.69 | 1.34 | 2.00 |

As mentioned in the previous section, the optimal dampers $\{\beta_{opt}\}$ for the PA model input can also be obtained by the same way as for the WN input. If we can predict the characteristics to some extent of future ground motions at the planning site, it could be more reasonable and effective to use the optimal dampers turned for the appropriately fitted PA model to the estimated ground motions. Thus, in this point of view, two types of dampers optimized for the WN and the PA model (denoted hereafter by WN-tuned and PA-tuned, respectively), are compared in Figure 5 on their effectiveness through their achieved equivalent damping factors under three types of input motions: the WN, the PA model, and the observed records (denoted hereafter by WN-input, PA-input, and OBS-input, respectively). The equivalent damping factor $h_{eq}$ for the OBS-input is calculated by using Eqn. (2.14) in which the ensemble average is replaced by the time average over the time required for the structure to dissipate 95% of the whole input energy.

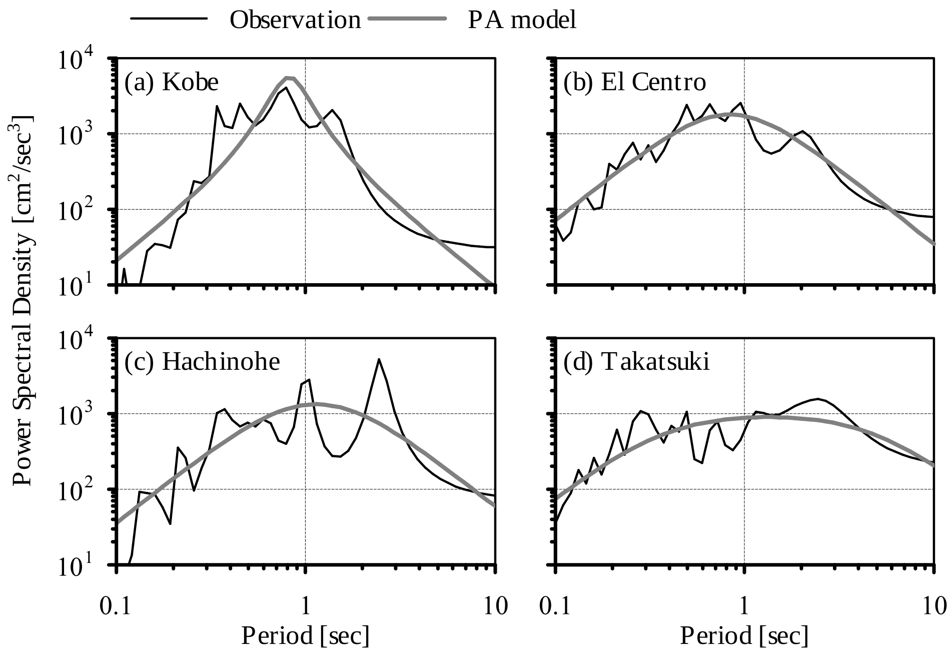


**Figure 4.** Power spectral density functions of sample ground motions

In Figure 5, the horizontal axis indicates the fundamental period $T_1$ of the five-story structural model. It is noted that the fundamental period have affects on the distribution of stiffnesses $\{K\}$ and therefore on the configuration of the optimal dampers $\{\beta_{opt}\}$. The WN-tuned dampers (denoted by circles) are always superior to the PA-tuned dampers (denoted by triangles) for the WN-input, and vice versa for the PA-input. However, those differences are not notable besides the case of (a) Kobe. This is supposed because the bandwidth of the Kobe record is relatively narrow as compared with those of other three records and the discrepancy from the WN is larger than others. It can be said that the WN-tuned dampers are effective even for non-WN input with reasonably wide bandwidth.

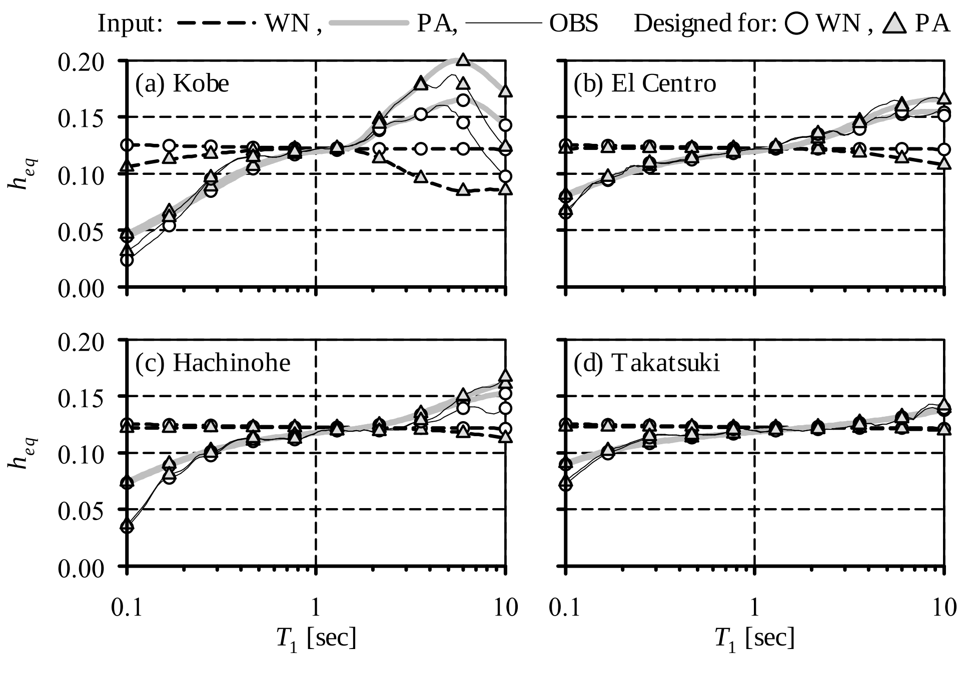


**Figure 5.** Equivalent damping factors for three types of input ground motion models

The $h_{eq}$ for the WN-input has almost a constant value over all $T_1$. On the other hand, the $h_{eq}$ for the PA-input has a tendency to increase with the increase of $T_1$. Each of the PA models has a predominant period $T_g = 2\pi / \omega_g$ of around 1.0 sec as shown in Table 3. If the fundamental period $T_1$ is longer than the predominant period $T_g$, the higher modes with periods shorter than $T_1$ are excited more strongly so that the predominant input energy at around $T_g$ is dissipated efficiently by those higher modes. In the case of $T_1 < T_g$, the higher modes make less contribution to the energy dissipation and induce the low damping factor.

Considering all the difference between the response spectrum of the observed records and that of the corresponding PA model, it can be said that the $h_{eq}$ for the PA-input gives a good approximation of that for the OBS-input as shown in Figure 5. It should be noted that the former is evaluated stochastically for the stationary response process, while the latter is for the non-stationary deterministic response process. Therefore, this also demonstrates that the optimal dampers tuned for the stationary stochastic input can work effectively for the non-stationary deterministic input.

## 4. CONCLUDING REMARKS

This paper presented the procedure to obtain the optimal configuration of Maxwell-type dampers installed in a multi-story structure so as to maximize the equivalent damping factor of the whole structural system. The equivalent damping factor as the objective function of the optimization is evaluated stochastically by the energy-consuming ratio during the stationary response process of the structure subjected to two types of random excitations: the WN with a flat spectrum and the PA model with a single predominant frequency. It was shown that the optimal dampers tuned for the WN input can also exhibit the efficiency under non-WN inputs with rather wide bandwidths. Moreover, it was found that the optimal distribution of non-dimensional damping coefficients of the Maxwell dampers is closely proportional to that of the stiffnesses of those spring elements. Finally, the effectiveness of the optimal dampers designed for a stationary random process was shown for non-stationary observed ground motions through the comparison between the expected and achieved equivalent damping factors.

**AKCNOWLEDGEMENT**
This work was partially supported by MEXT.KAKENHI(21560603).

## REFERENCES

BCJ (2011). The Building Standard Law of Japan on CD-ROM August 2011, The Building Center of Japan

Chen, Y.-T. and Chai, Y. H. (2010). Effects of brace stiffness on performance of structures with Supplemental Maxwell model-based brace–damper systems. *Earthquake Engineering and Structural Dynamics* **40**, 75-92.

Hatada, T., Kobori, T., Ishida, M. and Niwa, N. (2000). Dynamic analysis of structures with Maxwell model. *Earthquake Engineering and Structural Dynamics* **29**, 159-176.

Singh, M. P., Verma, N. P. and Moreschi, L. M. (2003). Seismic Analysis and Design with Maxwell Dampers. *Journal of Engineering Mechanics* **129:3**, 273-282.

Matsuda, S. and Asano, K. (2006). Analytical expression of earthquake input energy spectrum based on spectral density model of ground acceleration. *100th Anniversary Earthquake Conference Commemorating the 1906 San Francisco Earthquake*, 8NCEE-213.